FISEVIER

Contents lists available at ScienceDirect

Computers & Fluids

journal homepage: www.elsevier.com/locate/compfluid



Effects of free-slip boundary conditions on the flow around a curved circular cylinder



José P. Gallardo a,*, Bjørnar Pettersen a, Helge I. Andersson b

- ^a Department of Marine Technology, Norwegian University of Science and Technology, NO-7491 Trondheim, Norway
- ^b Department of Energy and Process Engineering, Norwegian University of Science and Technology, NO-7491 Trondheim, Norway

ARTICLE INFO

Article history:
Received 17 October 2012
Received in revised form 12 May 2013
Accepted 26 July 2013
Available online 5 August 2013

Keywords: Free-slip boundary conditions Curved circular cylinder Vortex shedding Wakes

ABSTRACT

Free-slip boundary conditions are routinely used in simulations of bluff body wakes without spanwise homogeneity. The impact of the free-slip condition on the wake behind a curved cylinder is considered. Inclusion of a six diameter long straight extension turned out to be sufficient to separate the adverse impact of free-slip from the curvature effects.

© 2013 Elsevier Ltd. All rights reserved.

1. Introduction

For the flow past a circular cylinder, it is well known that the physics are governed by the Reynolds number $Re \equiv U_\infty D/\nu$ [1], where U_∞ is the free stream velocity, D is the cylinder diameter and ν is the kinematic viscosity of the fluid. Many bluff body configurations, however, are more complex and introduce additional parameters governing the flow. Marine risers, for instance, are long flexible structures with circular cross-section which form a catenary curve as they hang freely in the ocean. This axial curvature together with the orientation of the bluff body with respect to the incoming flow are two additional parameters which affect the flow dynamics, as the numerical study of Miliou et al. [2] has shown. In their work, a fully three-dimensional approach was taken in order to investigate the mechanisms of vortex formation in the flow past a curved cylinder.

The numerical simulations in [2] were conducted at Re = 100 and 500 on two different flow configurations, both with the incoming flow aligned with the plane of curvature of the cylinder. On the first configuration the flow was directed towards the convex face of the curved cylinder (*convex* configuration). This resulted in fully three-dimensional shedding dynamics with one dominating shedding frequency. On the second configuration the flow was directed towards the concave face of the curved cylinder (*concave* configuration). This arrangement gave rise to strong axial flows which completely suppressed the vortex shedding. In both flow

configurations a free-slip boundary condition was prescribed at the location where the top end of the curved cylinder intersected the upper horizontal plane of the computational domain. The blockage effect due to this boundary condition was stronger in the concave configuration because the secondary flow stemming from the curvature of the cylinder was driven towards the top of the computational domain. Although the influence of the free-slip plane on the convex configuration was moderate in comparison, a free-slip plane inevitably inhibits vertical motions and thereby affects the vortex dynamics [3].

A natural extension of [2] is to increase the Reynolds number to study the flow dynamics when the wake is turbulent. For this purpose we recently studied the convex configuration at a Reynolds number of 3900 [4]. However, the formation of a tiny recirculation bubble just below the upper horizontal free-slip plane gave evidence of blocking effects, raising the question of whether it was necessary to extend the computational domain in the vertical direction. In the present work we intend to clarify this issue by reporting results from numerical simulations at Re = 3900. To this end, straight extensions of length 2D and 6D are appended to the top of the curved configuration studied in [2,4] in order to separate the influence of the upper free-slip boundary condition from the effects of curvature.

2. Problem definition and numerical methodology

2.1. Flow configuration

In the present investigation we use a bluff-body geometry identical to that studied by Miliou et al. [2] in its convex configuration.

^{*} Corresponding author. Tel.: +47 73551457; fax: +47 73595697. E-mail address: jose.p.gallardo@ntnu.no (J.P. Gallardo).

This consists of a quarter segment of a slender torus with aspect ratio R/D = 12.5, where R is the main radius of the torus and D the cylinder diameter (Fig. 1). At the lower-end of the bend, where the axis of the cylinder is aligned with the free-stream direction, a horizontal extension L_h = 10D is added in order to avoid end-effects, as shown in Fig. 1. Since the main objective of this work is to investigate the effect of the free-slip plane that truncates the upper-end of the curved cylinder, three different vertical extension lengths L_v are considered: no extension as in [2,4], an extension $L_v = 2D$ as the minimum length that could possibly isolate free-slip effects, and an extension of $L_v = 6D$ in order to check if dynamics of the flow past a straight circular cylinder are restored behind the vertical extension. The streamwise, cross-stream and vertical directions are herein denoted by x, y and z, respectively, and θ denotes the angle with vertex at the centre of the quarter-ring measured anticlockwise in the centreplane. The incoming flow is parallel to the x-direction and directed towards the convex face of the cylinder with a uniform velocity U_{∞} .

The Reynolds number is set to 3900 which, for a uniform circular cylinder, corresponds to the subcritical regime where the wake is turbulent and the free shear layers are unstable; see e.g. [5–7].

2.2. Numerical solution of the incompressible Navier-Stokes equations

The flow field is computed directly from the incompressible Navier–Stokes equations for a fluid with constant density and viscosity. We use the second-order finite volume code MGLET [8], which has been successfully used for DNS and LES of wall-bounded as well as free shear flows. The simulations are conducted on a staggered Cartesian grid with non-equidistant spacing in the three spatial directions. At the faces of the control volumes the velocities are obtained by linear interpolation, and a central-difference formulation approximates the first-order derivatives that arise from the diffusive terms in the momentum equation. The resulting discretized equations are integrated in time with an explicit low-storage third-order Runge–Kutta scheme [9]. At each of the three stages during time-integration a Poisson equation for pressure correction is solved iteratively using Stone's strongly implicit procedure (SIP) [10] with multigrid acceleration [8]. Domain decomposition in the

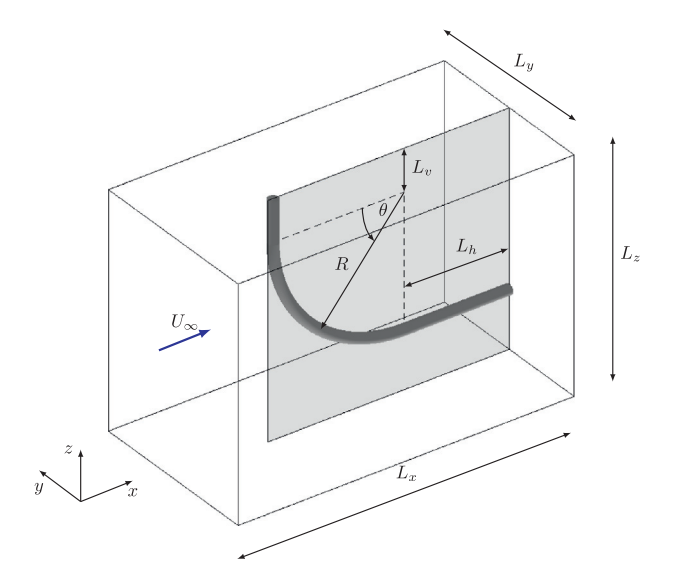


Fig. 1. Computational domain and geometry of the so-called convex configuration. The size of the computational domain is L_x , L_y and L_z in the x-, y- and z-directions, respectively. The quarter-of-ring has radius R, and is extended horizontally by L_h and vertically by L_v . In this paper, results taken at the gray-shaded symmetry (x,z)-plane are presented. Here, the streamwise coordinate of the baseline is given by $x_b = R - (R - D/2) \cos\theta$.

three Cartesian directions is implemented for parallelization. Representation of complex geometries inside the computational domain is taken into account by an immersed boundary method (IBM) [11]. This method relies on *direct forcing* to specify the non-slip and impermeability boundary conditions at the walls.

The computational domain in the horizontal (x,y)-plane is $L_x \times L_y = 38D \times 21D$ in the streamwise and cross-stream directions, respectively. In the vertical direction, the domain size L_z varies between 18D and 24D, depending on whether a vertical extension is added or not. Concerning grid resolution, the minimum grid spacing is dictated by the length scales in the very near wake and the gradients in the boundary layers. Typical resolutions in these regions in the horizontal (x,y)-plane are $\Delta x = 0.016D$ and $\Delta y = 0.008D$, and grid stretching is applied in the far field. These parameters lead to $N_x \times N_y = 1280 \times 448$ grid cells in the horizontal (x,y)-plane. In the vertical direction z a minimum grid spacing of $\Delta z = 0.028D$ is used, resulting in a total number of grid cells N_z of 512, 600 and 720, for the cases with no-extension, 2D-extension and 6D-extension, respectively. This resolution is based on the requirements to resolve spanwise structures in previous DNS and LES of the flow past a straight cylinder at Re = 3900 ([6,7]). In total, the number of grid cells amounts to 2.94×10^8 for the case without extension, 3.44×10^8 for 2D-extension, and 4.13×10^8 for 6Dextension. In order to check the resolution at different locations in the turbulent wake, the local grid size $\Delta = (\Delta x \Delta y \Delta z)^{1/3}$ is compared with the Kolmogorov length scale η obtained from the local dissipation rate of turbulent kinetic energy $\varepsilon = v \overline{\partial u_i / \partial x_i \partial u_i / \partial x_i}$, obtaining ratios Δ/η < 4 everywhere.

A constant time step of $\Delta t = 0.004 D/U_{\infty}$ is chosen to ensure a CFL number around 0.75. Simulations are first run for 750 convective time-units D/U_{∞} to allow for development of a quasi-periodic state and establishment of the secondary flows, after which statistics are collected for $600D/U_{\infty}$, or about 130 vortex shedding cycles.

2.3. Boundary conditions and free-slip effects

Our inflow boundary condition is a uniform velocity U_{∞} . At the outflow, a fully developed zero-stress condition consisting of a Neumann boundary condition for the velocity and pressure set to zero is prescribed. Free-slip boundary conditions are used at the vertical side planes, as well as at the top and bottom horizontal planes of the computational domain.

The primary effect of a free-slip boundary condition is the complete suppression of the velocity component perpendicular to the boundary. In the present context free-slip at the top horizontal plane is expressed as

$$w = 0$$
, $\frac{\partial u}{\partial z} = 0$, and $\frac{\partial v}{\partial z} = 0$. (1)

Although such free-slip boundary conditions affect the vortex dynamics in unsteady flows by imposing a kinematic blocking, they have been commonly used in computations involving complex geometries [12], non-uniform inflow [13,14], or a combination of both [15]. For conventional wakes Lamballais and Silvestrini [13] found that the main features of the wake dynamics were preserved by using free-slip boundary conditions. At the same time, free-slip planes were found to strongly affect the frequency selection in the wake behind a circular cylinder subjected to incoming linear shear flow [14].

For a curved cylinder in particular, Miliou et al. [2] discussed the effect of the artificial free-slip condition mostly in the concave configuration. Here a strong axial flow along the stagnation line was directed upwards towards the top-horizontal plane, and the blockage effect was more evident compared to the convex configuration, in which this flow was directed downwards. Our previous simulations at *Re* = 3900 [4], however, gave evidence of

Download English Version:

https://daneshyari.com/en/article/7157487

Download Persian Version:

https://daneshyari.com/article/7157487

<u>Daneshyari.com</u>